

Performance Evaluation of Timing Synchronization in OFDM-based Cognitive Radio Systems

Milan Zivkovic, Rudolf Mathar
Institute for Theoretical Information Technology,
RWTH Aachen University
D-52056 Aachen, Germany
Email: {zivkovic,mathar}@ti.rwth-aachen.de

Abstract—In this paper, the performance of Schmidl and Cox (S&C) timing estimator in cognitive radio systems under a fractional bandwidth (FBW) scenario is investigated. The synchronization preamble is appropriately modified in order to avoid transmission in the subbands where primary users (PU) are active. However, at the receiver, the timing synchronizer processes all received signal samples within the given OFDM band without any knowledge of a PU presence, thus being affected by interference. Statistical properties of timing metric in the presence of interference caused by PU are derived for an AWGN channel.

I. INTRODUCTION

According to recent studies, most of the licensed radio spectrum is severely underutilized in both the time and spatial domain [1]. Spectrum efficiency can be significantly increased by sharing the available frequency band between licensed primary users (PU) and a group of unlicensed secondary users or cognitive radios (CRs). By observing the spectrum of interest, CRs are able to detect the unused portions (*spectrum holes*) and adapt radio operation to dynamically changing environment without introducing harmful interference to the PU. In order to regulate opportunistic spectrum utilization, IEEE 802.22 working group puts efforts in standardization of wireless regional wireless networks (WRAN) providing broadband access in UHF/VHF TV bands between 54 and 862 MHz [2]. The standard also leaves opportunity that spectrum utilization methods can be extended within any regulatory regime.

Due to its flexibility in allocating resources among CRs, OFDM was shown as a promising candidate for physical (PHY) layer in WRAN standard. OFDM is a multicarrier modulation scheme that provides strong robustness against intersymbol interference (ISI) by dividing the broadband channel into many narrowband subchannels modulated on different subcarriers in such a way that attenuation across each subchannel stays flat. By leaving a set of subchannels unused, OFDM provides a flexible spectral shape that fills spectral gaps without interfering with the PU.

Various techniques for observation, decision, and action for CRs are currently being proposed in [2]. One of them is based on fractional bandwidth (FBW) usage where common bandwidth is divided into several subbands which can be activated (occupied by CRs) if spectrum sensing indicates the absence of PUs within them. During the initialization, the OFDM CR receiver needs to identify subbands which

This work has been partially supported by the UMIC Research Center, RWTH Aachen University.

are active and further process only the subcarriers in active subbands.

In order to obtain acceptable performance of OFDM receiver in FBW mode, it is necessary to find the correct start of the OFDM symbol by means of timing synchronization. An efficient and robust timing synchronization can be achieved by prepending several training symbols (preambles) of known data to the block of information data forming the data frame. Schmidl and Cox (S&C) proposed in [3] an efficient and robust method which is based on searching for the preamble with two identical halves in time domain. The beginning of the preamble corresponds to the peak value at the output of the correlator.

Although the opportunistic usage of common bandwidth in FBW mode preclude or try to minimize the mutual interference between PUs and CRs, timing synchronization is affected by interference presence in time domain since the CR receivers process all received samples in common dedicated bandwidth before the FBW detection. At this stage CR receiver does not distinguish CR signal in active subband from interfering SU signal. The presence of interference in non active subbands can considerable influence the performance of timing synchronization.

In [4] authors proposed the use of sufficiently long guard interval in the form of cyclic prefix which can provide intrinsic protection against ISI at the expense of some extra overhead. Previous works, found in literature, mostly analyzed the OFDM synchronization performance in the presence of narrowband interference (NBI). In [5], the influence of NBI, modeled as unmodulated complex sinusoid, on timing synchronization is investigated. The impact of digitally modulated NBI signals on the performance of S&C timing estimation is evaluated in [6]. In [7] authors investigated the influence of preamble subcarrier deactivation in occupied subbands on timing and frequency synchronization assuming that the interference is not present at the CR receiver.

The key contribution of this paper is the derivation of statistical properties of S&C timing estimator under FBW scenario in the presence of PU signal. Since CR's subcarriers deactivation in PU bands still preserves the time periodic structure of synchronization preamble introducing no interference to PU system, only the influence of PU interference to CR system can be harmful. The PU interference is modeled as additive Gaussian noise over subcarriers, as proposed in [8]. Additional assumption is that PU occupies all non active subbands with the same average power and that there is no mutual out of band transmission between PU and CR bands. Obtained results can be easily further extended by introducing

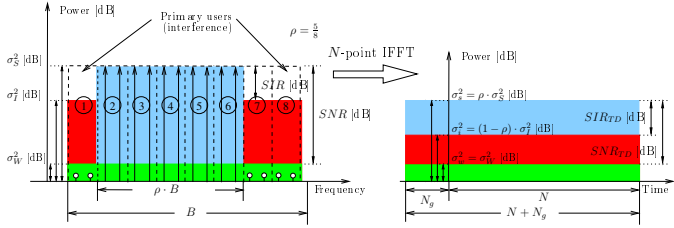


Fig. 1. Frequency and time representation of considered FBW model

filtering effects and arbitrary PU occupancy of the deactivated subbands.

The remainder of this paper is organized as follows. In Section II the FBW scenario is introduced and appropriate modification to synchronization preamble design is presented. Statistical properties of the timing metric of the S&C estimator in FBW mode in the presence of interference are derived in Section III. The analytical and simulation results are presented in Section V. Finally, some concluding remarks are given in Section VI.

II. SYSTEM MODEL

A. Fractional Bandwidth (FBW) Scenario

The FBW scenario where PUs and CR system share the common band B is shown in Fig. 1. The PU signals can appear on preassigned portion of the band or dynamically change the position within it. The CR transmitter obtains the information about spectrum occupancy from spectrum sensing and deactivate (null) the subcarriers in those subbands where PU signal is present. If the sensing results shows the change in spectrum occupancy, the proposed CR system can activate previously nulled subbands or null the subbands that were active. As shown in Fig. 1, the common frequency band B , consisting of N subcarriers, is divided into $M = 8$ subbands, each carrying $N_{BW} = N/M$ subcarriers. The total number of activated subbands can vary from 1 to M where only contiguous subbands are allowed to be activated in order to reduce the power leakage in the nulled subbands and mutual interference between PUs and CR [2]. Therefore, there are total $M_T = \frac{M(M+1)}{2}$ FBW modes with $M_A = 1, 2, \dots, M$ contiguous active subbands starting from the subband $M_S = 1, 2, \dots, M - M_A - 1$.

Define *pool allocation* as $\rho = M_A/M$ as a parameter which indicates the level of CR system spectrum utilization [7]. In the example shown in Fig. 1, with $M = 8$ subbands, the total $M_T = 36$ FBW modes are supported. There are $M_A = 5$ activated subbands, starting from $M_S = 2$ subband, thus giving the pool allocation of $\rho = \frac{5}{8} = 0.625$.

B. Transmission model

The block diagram of typical CR system in FBW scenario is shown in Fig. 2. Given the spectrum sensing results, the CR transmitter activates particular FBW mode m by only mapping the subcarriers of the active subbands of particular FBW mode while the rest of subcarriers is nulled. Let $C_m(n)$ denote the symbol carried on n th subcarrier in mode m , for $n = 0, \dots, N - 1$, while \mathcal{S}_m present the set of subcarriers belonging to active subbands. Therefore,

$$C_m(n) = \begin{cases} S(n), & n \in \mathcal{S}_m \\ 0, & n \notin \mathcal{S}_m \end{cases}, \quad (1)$$

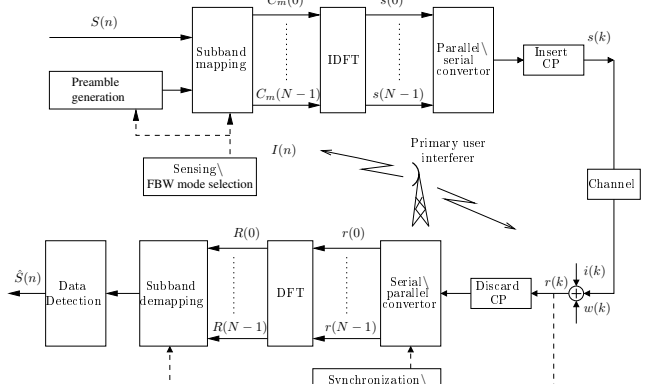


Fig. 2. The FBW system model

where $\sigma_S^2 = E\{|S(n)|^2\}$ is the average signal power. Without loss of generality in deriving statistical model for timing estimation performance, assume that all non active subbands are occupied with interference with same average power and that there is no interference power leakage to active subbands. The interference on subcarriers is modeled as sampled complex zero-mean Gaussian random variable with zero mean and variance σ_I^2 , i.e., $I(n) \sim \mathcal{N}(0, \sigma_I^2)$ [8], giving

$$I_m(n) = \begin{cases} 0, & n \in \mathcal{S}_m \\ I(n), & n \notin \mathcal{S}_m \end{cases}. \quad (2)$$

Furthermore, noise samples are modeled as complex zero-mean AWGN, $W(n)$, with variance σ_W^2 , i.e. $W(n) \sim \mathcal{N}(0, \sigma_W^2)$. To simplify the ongoing analysis, without losing generality, an AWGN channel is considered, which is a regular assumption since S&C is robust to multipath propagation if the CP is sufficiently large. The spectral content on the subcarriers within the common bandwidth can be then written as

$$R(n) = \begin{cases} S(n) + W(n), & n \in \mathcal{S}_m \\ I(n) + W(n), & n \notin \mathcal{S}_m \end{cases}. \quad (3)$$

Let N_g denote the number of samples in cyclic prefix. The received signal received signal in time domain $r(k)$, after the ADC conversion and prior to time estimation, for $k = -N_g, \dots, N - 1$ is given as

$$\begin{aligned} r(k) &= \frac{1}{N} \sum_{n=0}^{N-1} R(n) e^{-j2\pi \frac{nk}{N}} \\ &= \frac{1}{N} \left(\sum_{n \in \mathcal{S}_m} S(n) + \sum_{n \notin \mathcal{S}_m} I(n) + \sum_{n=0}^{N-1} W(n) \right) e^{-j2\pi \frac{nk}{N}} \\ &= s(k) + i(k) + w(k). \end{aligned} \quad (4)$$

Since only subcarriers in active subbands which belong to mode m are loaded, the average signal power in time domain is scaled with pool allocation, thus giving $\sigma_s^2 = E\{|s(k)|^2\} = \rho \sigma_S^2$. Similarly, the average interference power in time domain can be written as $\sigma_i^2 = E\{|i(k)|^2\} = (1 - \rho) \sigma_I^2$ while the average noise power stays the same $\sigma_w^2 = E\{|w(k)|^2\} = \sigma_W^2$. Therefore, we can define the frequency domain average signal-to-noise ratio (SNR) of the received signal in active subbands

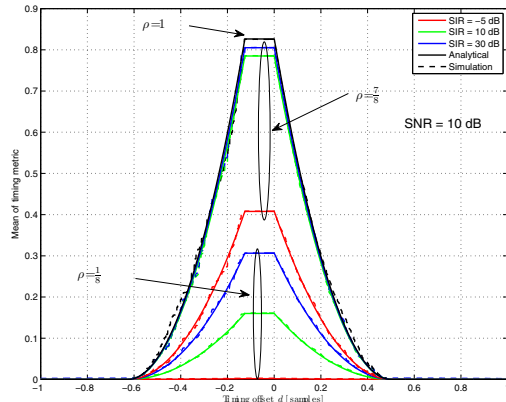


Fig. 3. Mean timing metric at $\text{SNR} = 10 \text{ dB}$

as

$$\text{SNR} = \frac{\sigma_s^2}{\sigma_w^2}, \quad (5)$$

while the average SNR in time domain is given as

$$\text{SNR}_{TD} = \frac{\sigma_s^2}{\sigma_i^2} = \rho \text{SNR}. \quad (6)$$

Although desired signal and interference are separated within common band B , as shown in Fig. 1, let's define the ratio between average signal power and average interference power as the average signal-to-interference ratio (SIR), written as

$$\text{SIR} = \frac{\sigma_s^2}{\sigma_i^2}, \quad (7)$$

while the average SIR in time domain is given as

$$\text{SIR}_{TD} = \frac{\sigma_s^2}{\sigma_i^2} = \frac{\rho}{(1-\rho)} \text{SIR}. \quad (8)$$

The visual representation of above defined quantities and their relations both in the frequency and time domain is shown in Fig. 1.

C. Preamble design

In many wireless OFDM systems, transmission is normally organized in frames where sequence of data symbols is preceded by several preambles of known data used for the synchronization and/or channel estimation purposes. Performing timing estimation, the S&C algorithm utilizes the time periodic structure of the first preamble which contains two identical halves prepended by CP in order to make system robust to multipath propagation. Therefore, the time domain representation of the preamble can be written as

$$s_p(k) = s_p(k + N/2), \quad k = 0, \dots, \frac{N}{2} - 1, \quad (9)$$

which can be formed in frequency domain by transmitting QPSK or PN sequence on the even subcarriers in the active subbands, thus giving

$$C_{m,p}(n) = \begin{cases} \sqrt{2}S_p(n), & n \in \mathcal{S}_{p,m}, \\ 0, & n \notin \mathcal{S}_{p,m} \end{cases}, \quad (10)$$

where $\mathcal{S}_{p,m}$ presents the set of even subcarriers belonging to active subbands of mode m , i.e., $\mathcal{S}_{p,m} \subset \mathcal{S}_m$ while scaling factor $\sqrt{2}$ is used to preserve average signal energy.

III. STATISTICAL PROPERTIES OF THE TIMING METRIC

The S&C timing estimation algorithm is based on searching for the correlation peak between the input samples separated by half of one OFDM symbol, which coincides with the start of synchronization preamble [3]. From (4), the received preamble in time domain can be written as

$$r_p(k) = s_p(k) + i_p(k) + w_p(k). \quad (11)$$

In order to simplify further notation, index p will be omitted since we consider only statistical properties of synchronization preamble. The symbol timing estimator searches for the instant d , where the timing metric

$$M(d) = \frac{|P(d)|^2}{R(d)} \quad (12)$$

reaches its maximum, which corresponds to the start of the frame, while $P(d)$ and $R(d)$ are given by

$$P(d) = \sum_{k=0}^{N/2-1} r^*(d+k) \cdot r(d+k + \frac{N}{2}) \quad (13)$$

and

$$R(d) = \sum_{k=0}^{N/2-1} |r(d+k + \frac{N}{2})|^2. \quad (14)$$

If the timing metric $M(d)$ exceeds a predetermined threshold T estimator decides that it is possible to detect a training sequence, otherwise, preamble is not detected. The important issue is to find a value of threshold such that the probability of missing a training symbol when there is one present, and the probability of falsely detecting a training sequence when there is none present be as small as possible.

To find these probabilities we need to determine statistical properties of the timing metric. In [3], statistical properties of the timing metric at the optimum timing point and at a position outside the preamble were investigated. In [6], statistical properties of the S&C timing metric in the presence of NBI are presented. Here, we extend the previous results in order to obtain statistical properties of the timing metric in the presence of interference in FBW mode.

To find mean and variance of the estimator at best symbol timing, first look at $P(d)$, which after replacing (11) and (9) in (13), can be written as

$$P(d_{opt}) = \sum_{k=0}^{N/2-1} s^*(d+k) \cdot r(d+k + \frac{N}{2}) + \sum_{k=0}^{N/2-1} (i^*(d+k) + w^*(d+k)) \cdot r(d+k + \frac{N}{2}).$$

Similarly, $R(d)$ is given as

$$R(d_{opt}) = \sum_{k=0}^{N/2-1} s^*(d+k) \cdot r(d+k + \frac{N}{2}) + \sum_{k=0}^{N/2-1} [(i^*(d+k + \frac{N}{2}) + w^*(d+k + \frac{N}{2})) \cdot r(d+k + \frac{N}{2})].$$

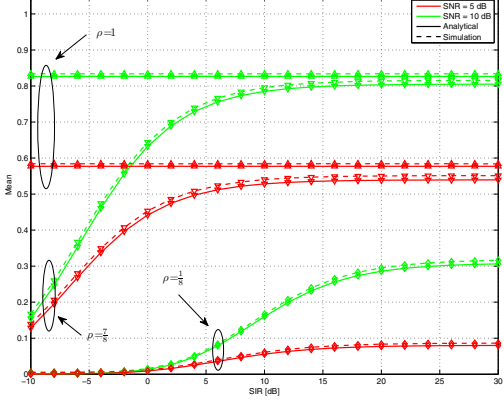


Fig. 4. Mean of timing metric at optimum point for $N = 2048$.

It can be noticed that both metrics have common part. For high values of SNR and SIR, magnitude of $|P(d_{opt})|$ and $R(d_{opt})$ can be approximated by their real parts, since imaginary part can be neglected. Therefore, $|P(d_{opt})| \approx \text{Real}\{P(d_{opt})\} = a + b$ and $R(d_{opt}) \approx \text{Real}\{R(d_{opt})\} = a + c$, where a is

$$a = \sum_{k=0}^{N/2-1} |s(d+k)|^2 + \sum_{k=0}^{N/2-1} \text{Real} \left\{ s^*(d+k) \cdot (i(d+k + \frac{N}{2}) + w(d+k + \frac{N}{2})) \right\}.$$

According to central limit theorem (CLT), a is Gaussian random variable with its expected value $\mu_a = N \cdot \sigma_s^2$. Similarly,

$$b = \sum_{k=0}^{N/2-1} \text{Real} \left\{ (i^*(d+k) + w^*(d+k)) \cdot r(d+k + \frac{N}{2}) \right\}.$$

is Gaussian random variable with zero mean, $\mu_b = 0$, and variance $\sigma_b^2 = N \cdot (\sigma_w^2(\sigma_s^2 + \sigma_w^2) + \sigma_i^2(\sigma_s^2 + \sigma_i^2 + 2\sigma_w^2))$, while

$$c = \sum_{k=0}^{N/2-1} \text{Real} \left\{ (i^*(d+k + \frac{N}{2}) + w^*(d+k + \frac{N}{2})) \cdot r(d+k + \frac{N}{2}) \right\}$$

is also Gaussian random variable with mean value $\mu_c = N \cdot \sigma_w^2 + N \cdot \sigma_i^2$ and variance $\sigma_c^2 = N \cdot (\sigma_w^2(\sigma_s^2 + 2\sigma_w^2) + \sigma_i^2(\sigma_s^2 + 2\sigma_i^2 + 4\sigma_w^2))$. The square root of the timing metric at optimal timing point, $M(d_{opt})$, is defined as $q = |P(d_{opt})|/R(d)$. Let's assume that at high SNR and SIR values, for both numerator and denominator of q , standard deviations are much smaller than the averages. Therefore, q can be approximated by a Gaussian variable [9] with mean and variance given by the following approximations

$$\mu_q = \frac{\mu_a + \mu_b}{\mu_a + \mu_c}, \quad (15)$$

$$\sigma_q^2 = \mu_q^2 \left(\frac{\sigma_b^2}{(\mu_a + \mu_b)^2} + \frac{\sigma_c^2}{(\mu_a + \mu_c)^2} \right). \quad (16)$$

Taking into account that q is approximately a Gaussian random variable, and $M(d_{opt})$ is the square of q , it follows that $M(d_{opt})$ is also approximately a Gaussian variable $M(d_{opt}) =$

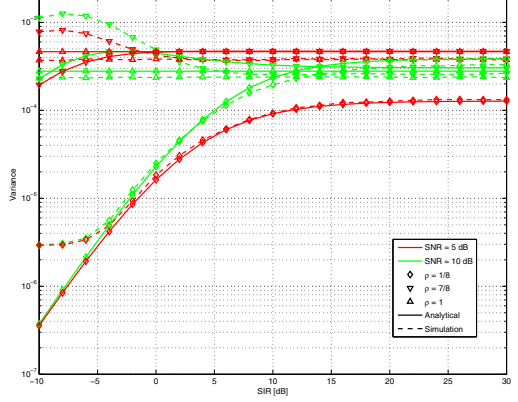


Fig. 5. Variance of timing metric at optimum point for $N = 2048$.

$(\mu_q + \mathcal{N}(0, \sigma_q^2))^2 \approx \mu_q^2 + 2\mu_q\mathcal{N}(0, \sigma_q^2)$ with mean value $\mu_M = E\{M(d_{opt})\} = \mu_q^2$ which can be derived as

$$\begin{aligned} \mu_M &= \left(\frac{\sigma_s^2}{\sigma_s^2 + \sigma_i^2 + \sigma_w^2} \right)^2 \\ &= \left(\frac{1}{1 + \frac{1}{SNR_{TD}} + \frac{1}{SIR_{TD}}} \right)^2 = \left(\frac{1}{1+x} \right)^2 \end{aligned} \quad (17)$$

where

$$x = x(SNR, SIR, \rho) = \frac{1}{\rho SNR} + \frac{1-\rho}{\rho SIR}. \quad (18)$$

Similarly, variance is derived as [3]

$$\begin{aligned} \sigma_M^2 &= 4\mu_q^2\sigma_q^2 \\ &= \frac{4\sigma_s^4((1+\mu_M)\sigma_s^2(\sigma_i^2 + \sigma_w^2) + (1+2\mu_M)(\sigma_i^2 + \sigma_w^2)^2)}{N(\sigma_s^2 + \sigma_i^2 + \sigma_w^2)^4} \\ &= \frac{4x}{N(1+x)^3} \left(1 + \frac{1+2x}{(1+x)^3} \right). \end{aligned}$$

Considering the statistical properties of a timing position d outside of the training sequence in FBW scenario, an analysis similar to one given in [3] and [6] can be conducted. It can easily be verified that for sufficiently large SNR and SIR values, the timing metric can be approximated by a chi-square distributed random variable, thus giving

$$M(d_{out}) = \frac{\chi_2^2}{N} \quad (19)$$

where χ_2^2 is a chi-square-distributed random variable with two degrees of freedom and its mean and variance equal to 2 and 4, respectively. Therefore, the mean and the variance of $M(d_{outside})$ can be written as $\mu_M(d_{out}) = \frac{2}{N}$ and $\sigma_M^2(d_{out}) = \frac{4}{N^2}$, respectively. The mean value of timing metric is then given as

$$\mu_M(d) = \begin{cases} \frac{(2(d+N_g + \frac{N}{2}))^2}{(N(1+x))^2}, & -(\frac{N}{2} + N_g) < d \leq -N_g \\ \frac{1}{(1+x)^2}, & -N_g < d \leq 0 \\ \frac{(2(-d + \frac{N}{2}))^2}{(N(1+x))^2}, & 0 < d \leq \frac{N}{2} - 1 \\ \frac{2}{N}, & \text{otherwise,} \end{cases}$$

which is shown in Fig. 3 jointly with simulation results for SNR = 10 dB and different SIR values and various pool

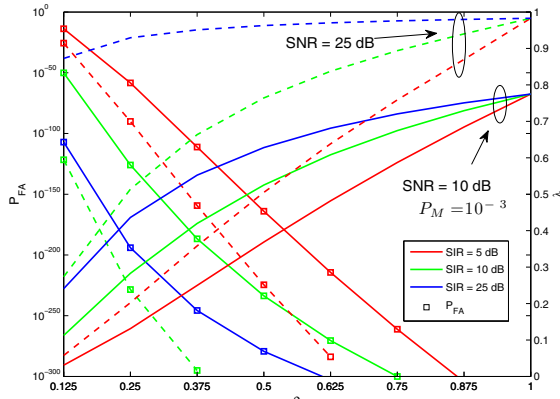


Fig. 6. P_{FA} and required maximal threshold λ for given $P_M = 10^{-3}$.

allocations ρ . It can be seen that maximum timing metric forms a plateau whose length is preserved for all SIR values. Although the plateau produces ambiguity of correct timing point detection which can be corrected by equalization, it also provides protection margin in frequency selective channels. It is shown that this margin is not affected by actual pool allocation and SIR value. However, the maximum timing metric is decreasing when SIR and pool allocation decrease, thus increasing probability of missing preamble presence. It can be observed that even in the presence of strong interference, when $SIR = -5$ dB, and high pool allocation of $\rho = 7/8$ synchronizer provides better performance compared to low pool allocation $\rho = 1/8$ and $SIR = 30$ dB. Therefore, it can be concluded that actual spectrum occupancy is more critical for system performance.

IV. MISSING AND FALSE DETECTION PROBABILITY

Statistical properties of timing metric calculated in previous section can be used to determine both the probability of not detecting a training sequence when one is present (P_M) and of falsely detecting a training sequence when one is not present (P_{FA}). Let us define the threshold λ which is compared to metric $M(d)$ in order to determine the presence of the preamble. As shown in [9], $P_M(\lambda)$ can be written as

$$P_M(\lambda) = \frac{1}{2} \operatorname{erfc} \left(\frac{\mu_M - \lambda}{\sqrt{2\sigma_M^2}} \right) \quad (20)$$

where $\operatorname{erfc}(x) = 2/(\sqrt{\pi}) \int_x^\infty e^{-z^2} dz$. Similarly, $P_{FA}(\lambda)$ can be derived as

$$P_{FA}(\lambda) = e^{-\lambda N/2}. \quad (21)$$

V. PERFORMANCE EVALUATION

In order to investigate the influence of different pool allocations and interference powers on the performance of S&C time synchronization algorithm in cognitive radio systems under FBW scenario, numerical and simulation results are obtained. The CR channel is considered as AWGN, without loss of generality, since the algorithm was shown to be robust to multipath propagation if the CP is sufficiently large. However, the straightforward extension to other types of channels can be conducted. It is further assumed that the total number of subcarriers is 2048 according to WRAN standard proposal [2].

Fig. 4 shows the mean of timing metric at the optimum timing point as a function of SIR for SNR and pool allocation as parameters. It can be observed that the simulation results

agree with the analytical expressions. It is shown that at large SIR values, timing metric reaches an asymptote determined by the actual SNR value and pool allocation, while the lower pool allocation requires higher SIR for reaching particular asymptote.

The variance of the timing metric at the optimum timing point as a function of SIR for SNR and pool allocation as parameters is shown in Fig. 5. Again, the simulation curves correspond with the analytical results in large SIR region. The simulation performance differs from analytical results at low SIR values due to high SNR and SIR assumptions made during development of analytical model.

Fig. 6 depicts the required thresholds λ for achieving probability of miss $P_M = 10^{-3}$ obtained from (20) and corresponding probability of false detection P_{FA} derived from (21) as a function of pool allocation given the SIR and SNR as parameters. The required threshold for given P_M increases with the pool allocation and is getting larger for higher SNR and SIR values. Accordingly, P_{FA} for required threshold and given P_M decreases with pool allocation and becomes lower for higher SNR and SIR values.

VI. CONCLUSION

This paper investigates the performance of S&C timing estimator [3] in cognitive radio systems under FBW scenario. The synchronization preamble was appropriately modified in order to avoid transmission in the subbands where PU is active. Statistical properties of timing metric in the presence of interference caused by PU are derived for an AWGN channel. Numerical expressions for mean and variance of timing metric corresponds to simulation results for large regions of SNR and SIR. It is shown that actual spectrum occupancy is more critical for system performance compared to SIR values. At large SIR values, timing metric reaches an asymptote determined by the actual SNR value and pool allocation. The increase of pool allocation increases the average timing metric. Finally, analytical results for required threshold for achieving certain probability of miss P_M and corresponding probability of false detection P_{FA} show that for higher SNR and SIR values threshold increases faster with the pool allocation while P_{FA} rapidly decreases with pool allocation.

REFERENCES

- [1] I. Mitola, J. and J. Maguire, G.Q., "Cognitive radio: making software radios more personal," *IEEE Pers. Commun.*, vol. 6, no. 4, pp. 13–18, Aug. 1999.
- [2] J. Benko, S.-Y. Chang, and Y.-C. Cheong, "Draft PHY/MAC specification for ieee 802.22," IEEE 802.22-06/0069r1, Tech. Rep., 2006.
- [3] T. Schmidl and D. Cox, "Robust frequency and timing synchronization for OFDM," *IEEE Trans. Commun.*, vol. 45, no. 12, pp. 1613–1621, Dec 1997.
- [4] T. Weiss, A. Krohn, F. Capar, I. Martoyo, and F. K. Jondral, "Synchronization algorithms and preamble concepts for spectrum pooling systems," *IST Mobile & Wireless TeleCommun. Summit*, June 2003.
- [5] A. Coulson, "Narrowband interference in pilot symbol assisted OFDM systems," *IEEE Trans. Wireless Commun.*, vol. 3, no. 6, pp. 2277 – 2287, nov. 2004.
- [6] M. Marey and H. Steendam, "Analysis of the narrowband interference effect on OFDM timing synchronization," *IEEE Trans. Sig. Proc.*, vol. 55, no. 9, pp. 4558–4566, 2007.
- [7] M. Krondorf, T.-J. Liang, and G. Fettweis, "On synchronization of opportunistic radio OFDM systems." *Proc. of IEEE VTC 2008 Spring*, pp. 1686–1690, 2008.
- [8] T. Yucek and H. Arslan, "MMSE noise plus interference power estimation in adaptive OFDM systems," *IEEE Trans. Veh. Technol.*, vol. 56, no. 6, pp. 3857 –3863, Nov. 2007.
- [9] R. Walpole and M. Raymond, *Probability & statistics for engineers & scientists*, 8th ed. Upper Saddle River, NJ: Pearson/Prentice Hall, 2007.